Conf-911111--22

PNL-SA--19385

DE92 006518

DISCLAIMER

DETERMINATION OF CREEP COMPLIANCE AND CREEP-SWELLING COUPLING COEFFICIENTS FOR NEUTRON-IRRADIATED TITANIUM-MODIFIED STAINLESS STEEL AT 400°C

F. A. Garner
M. B. Toloczko
C. R. Eiholzer

November 1991

Presented at the
5th International Conference on
Fusion Reactor Materials
November 17-22, 1991
Clearwater, Florida

Work supported by
the U.S. Department of Energy
under Contract DE-AC06-76RLO 1830

Pacific Northwest Laboratory
Richland, Washington 99352

MASTER

DETERMINATION OF THE CREEP COMPLIANCE AND CREEP-SWELLING COUPLING COEFFICIENT FOR NEUTRON IRRADIATED TITANIUM-MODIFIED STAINLESS STEELS AT ~400°C - M. B. Toloczko, University of California at Berkeley, F. A. Garner, Pacific Northwest Laboratory,[a] and C. R. Eiholzer, Westinghouse Hanford Company

OBJECTIVE

The objective of this effort is to provide irradiation creep data and design correlations for application to fusion and breeder reactor design.

SUMMARY

Irradiation creep data from FFTF-MOTA at ~400°C were analyzed for nine 20% cold-worked titanium-modified type 316 stainless steels, each of which exhibits a different duration for the transient regime of swelling. One of these steels was the fusion prime candidate alloy designated PCA. The others were various developmental breeder reactor heats. The analysis was based on the assumption that the B_o + DS creep model applies to these steels at this temperature. This assumption was found to be valid. A creep-swelling coupling coefficient of $D \approx 0.6 \times 10^{-2}$ MPa^{-1} was found for all steels that had developed a significant level of swelling. This result is in excellent agreement with the results of earlier studies conducted in EBR-II using annealed AISI 304L and also 10% and 20% cold-worked AISI 316 stainless steels. There appears to be some enhancement of swelling by stress, contradicting an important assumption in the analysis and leading to an apparent but misleading nonlinearity of creep with respect to stress.

PROGRESS AND STATUS

Introduction

In a number of recent reports the creep-swelling relationship has been investigated for annealed AISI 304L[1] and various thermomechanical treatments of AISI 316 stainless steel.[2-6] These studies were conducted in EBR-II and showed a remarkable consistency in results, indicating that irradiation creep at most temperatures of interest could be described as consisting of several minor contributions (precipitation-related dimensional changes and transient relaxation of cold-work-induced dislocations) and two major contributions.[6] The major contributions were associated with the creep compliance, B_o, a quantity unrelated to void swelling, and a swelling-driven creep component. Although swelling itself is very sensitive to a large variety of material and environmental variables, the instantaneous creep rate appears to be proportional only to the applied stress and the instantaneous swelling rate. As discussed in other publications,[7-9] the instantaneous creep rate can be written in the form

$$B = \dot{\bar{\epsilon}}/\bar{\sigma} = B_o + D\dot{S}, \tag{1}$$

where $\dot{\bar{\epsilon}}/\bar{\sigma}$ is the effective strain rate per unit stress, $\bar{\sigma}$ is the effective stress = $(\sqrt{3}/2)\ \sigma_{hoop}$, B_o is the creep compliance, D is the creep-swelling coupling coefficient and $\dot{S}$ is the instantaneous volumetric swelling rate. This equation applies primarily to annealed material that does not develop any significant phase-related strains or density changes. Type 316 stainless steels are known to exhibit density changes, however, arising from carbide precipitation[10] and formation of intermetallic phases.[11] If the material is cold-worked, another short-lived transient term is sometimes required to describe the relaxation of the dislocation density to its equilibrium level.

Experimental Details

In this study, the fusion prime candidate alloy (PCA heat K280) and eight other titanium-modified type 316 steels from the breeder reactor program were irradiated in FFTF/MOTA. For three of the alloys, 2.24-cm-long helium-pressurized tubes were used with outer and inner diameters of 4.57 mm and 4.17 mm, respectively. The other six alloys had tubes that were somewhat larger, with a length of 2.82 cm, and 5.84 and 5.08 mm outer and inner diameters. The difference in size alone does not influence the creep results.[12] The compositions of these steels are shown in Table I. The specimens were removed periodically from the reactor and their diameters measured at five equidistant positions using a noncontacting laser system.[13] The three middle measurements were averaged to calculate the diametral strain. During any one irradiation interval the temperature is actively controlled within ±5°C. The tubes for any one alloy were placed side-by-side in

(a) Pacific Northwest Laboratory is operated for the U.S. Department of Energy by Battelle Memorial Institute under Contract DE-AC06-76RLO 1830.

Table 1. Composition (wt%) of Stainless Steels Used in this Study

Heat	Fe	Ni	Cr	Mo	Mn	Si	C	P	Ta	Zr
K280	BAL	16.63	14.31	1.95	1.83	0.52	0.048	0.014	--	--
83508*	BAL	15.77	13.70	1.65	2.03	0.80	0.039	<0.005	<0.01	<0.01
A094*	BAL	15.64	13.34	2.21	1.52	0.81	0.038	0.040	--	--
A095*	BAL	15.59	13.58	1.81	1.62	0.82	0.038	0.038	--	--
C38	BAL	15.60	13.66	1.82	2.20	0.82	0.048	0.032	<0.010	--
C39	BAL	15.59	13.59	1.82	2.19	0.78	0.048	0.088	<0.008	--
C40	BAL	15.60	13.63	1.81	2.20	0.81	0.044	0.088	<0.008	--
C42	BAL	15.79	13.62	1.81	2.30	0.81	0.049	0.030	<0.010	--
C44	BAL	20.08	13.64	1.80	2.30	0.83	0.046	0.032	<0.016	--

Continued:

Heat	S	V	Nb	Ti	Co	Cu	Al	B	N
K280	0.025	0.04	0.02	0.31	0.04	0.02	0.05	0.001	0.008
83508*	0.003	0.01	--	0.34	<0.01	<0.01	<0.01	0.0005	0.004
A094*	0.009	0.020	--	0.28	0.05	0.02	<0.01	0.0041	0.006
A095*	0.008	0.011	--	0.28	0.04	0.02	<0.01	0.0047	0.003
C38	0.004	0.03	<0.010	0.27	0.03	0.02	0.03	0.0033	0.002
C39	0.004	0.03	<0.008	0.27	0.03	0.02	0.03	0.0029	0.005
C40	0.006	0.02	<0.008	0.27	0.03	0.01	0.03	0.0064	0.006
C42	0.005	0.02	<0.010	0.26	0.03	<0.01	0.03	0.0062	0.002
C44	0.005	0.02	<0.016	0.26	0.03	0.02	0.03	0.0061	0.004

* These heats have a tube size of 5.84mm OD x 5.08mm ID x 28.2mm in Length. All others are 4.57mm OD x 4.17mm ID x 22.4mm in Length.

MOTA although different alloy sets experienced slightly different temperatures and neutron fluxes. For each group of tubes there were small cycle-to-cycle variations in temperature and neutron flux that arose as the group of tubes were placed at somewhat different reactor levels following each MOTA reconstitution (see Table 2). Preliminary results for PCA and one of the breeder reactor alloys have been reported previously.[14]

Results and Discussion

Figure 1 shows for three alloys the total diametral strains for nominally identical tubes irradiated side-by-side for a number of consecutive FFTF irradiation cycles at ~400°C. The data for the other six alloys are very similar, varying only the duration of the transient regime of deformation. The separate tubes of each alloy varied only in their internal gas pressure, which yielded hoop stresses ranging from 0 to 300 MPa. Note that these data are plotted against the neutron exposures expressed in units of dpa. An earlier report contained the data for PCA as a function of neutron fluence for energies greater than 0.1 MeV.[15] Both the neutron fluence and dpa values for the first several irradiation segments have been revised recently. The revised values are reported in Table 2.

The diameter changes of the zero stress tubes represent primarily the contribution of void swelling, but there may also be some secondary contribution from precipitation-related strains. The strains of the stressed tubes include additional contributions from irradiation creep and possibly the stress-enhanced portion of swelling, since applied stresses are known to accelerate the onset of swelling.[16-18] Figure 2 shows the diametral strains of the stress free tubes for all nine alloys, indicating that the transient regime of swelling varies somewhat with composition, fabrication history, and irradiation conditions.

In order for the creep data to fit the $B_o + D\dot{S}$ model, it is necessary for creep to be proportional to the first power of stress and to increase directly in proportion to the instantaneous swelling rate. If we calculate the midwall creep strains and divide them by the stress level, the validity of these assumptions can be checked. First, the creep strains are separated by subtracting the zero stress swelling strains. Figure 3 presents a comparison of the stress-normalized midwall strains for three steels. The latter figure shows that each of the steels exhibits accelerated creep rates that coincide with the onset of accelerated swelling, but that the stress-normalized creep strains do not appear to be completely linear with applied stress. However, this appearance is probably misleading, with the slight but steady increase in normalized creep strain with increasing stress arising from the somewhat incorrect assumption that swelling is not affected by stress. (Similar trends were observed in the other six steels.) In general, increasing the stress level progressively shortens the incubation period of swelling in cold-worked austenitic steels.[16-18] It appears in this study that there is also a small but persistent effect of stress on the incubation period of swelling.

Table 2. Irradiation History of Each Heat

	MOTA - 1A	MOTA - 1B	MOTA - 1C	MOTA - 1D	MOTA - 1E	MOTA - 1F
K280 (PCA)						
Canister/Basket	1D3	1D5	1F5	1F5	1F5	1F1
Temp., °C	405	401	396	386	384	386
Φ_t, x10^{22} n/cm^2 (E>0.1MeV)	4.6	6.6	11.9	15.4	19.2	24.8
Cumulative dpa	20.4	29.3	50.2	65.3	81.1	106.8
83508 (D9 Reference)						
Canister/Basket	2F1	2F2	2F2	2F4	absent	absent
Temp., °C	427	431	420	404		
Φ_t, x10^{22} n/cm^2 (E>0.1MeV)	6.0	9.2	16.7	21.9		
Cumulative dpa	27.8	42.6	77.2	101.2		
A094 (D9I - 2)						
Canister/Basket	absent	2F4	2F4	2F2	2F1	2F4
Temp., °C		431	420	410	410	410
Φ_t, x10^{22} n/cm^2 (E>0.1MeV)		3.1	10.3	15.7	23.7	30.6
Cumulative dpa		14.1	47.2	72.2	109.2	141.2
A095 (D9I - 1)						
Canister/Basket	absent	2F3	2F3	2F1	2F3	2F4
Temp., °C		431	420	410	410	410
Φ_t, x10^{22} n/cm^2 (E>0.1MeV)		3.1	10.5	16.0	23.4	30.3
Cumulative dpa		14.5	48.4	73.9	108.1	140.1
C38 (D9 B/P - 1)						
Canister/Basket	absent	1D2	1F5/1F4	1F2	1F2	1F6
Temp., °C		401	396	386	384	386
Φ_t, x10^{22} n/cm^2 (E>0.1MeV)		2.6	7.7	12.1	17.4	20.6
Cumulative dpa		11.5	32.4	52.3	76.5	89.8
C39 (D9 B/P - 2)						
Canister/Basket	absent	1D3	1F3	1F2	1F2	1F6
Temp., °C		401	396	386	384	386
Φ_t, x10^{22} n/cm^2 (E>0.1MeV)		2.4	8.0	12.4	17.7	20.9
Cumulative dpa		10.6	35.5	55.4	79.6	92.9
C40 (D9 B/P - 3)						
Canister/Basket	absent	1D3	1F3	1F3	1F3	1F6
Temp., °C		401	396	386	384	386
Φ_t, x10^{22} n/cm^2 (E>0.1MeV)		2.4	8.0	12.2	17.0	20.2
Cumulative dpa		10.6	35.5	54.1	75.7	89.0
C42 (D9 B/P - 4)						
Canister/Basket	absent	2F4	2F4	2F5	2F3	2F3
Temp., °C		431	420	404	414	405
Φ_t, x10^{22} n/cm^2 (E>0.1MeV)		3.1	10.3	15.4	22.8	30.1
Cumulative dpa		14.1	47.2	70.5	104.7	138.5
C44 (D9 B/P - 5)						
Canister/Basket	absent	1D3	1F3	1F2	1F2	1F6
Temp., °C		401	396	386	384	386
Φ_t, x10^{22} n/cm^2 (E>0.1MeV)		2.4	8.0	12.4	17.7	20.9
Cumulative dpa		10.6	35.5	55.4	79.6	92.9

The PCA (heat K280) alloy at the somewhat lower displacement rate and irradiation temperature is clearly swelling and creeping at rates comparable to that of the 83508 alloy at a slightly higher displacement rate and temperature, but the onset of accelerated strain rate occurs with a delay of ~10 dpa relative to that of 83508. This delay cannot be attributed to compositional differences alone, but probably arises in part from both compositional and environmental differences (displacement rate and temperature). It may also reflect some differences in production methods associated with the two types of tubes.[12] Compared to the behavior of PCA and heat 83508, the A095 heat exhibits an even longer transient in both creep and swelling.

If both the small effect of stress on swelling and the possibility of precipitation-related strains are ignored, one can calculate a first order estimate of the B_o and D coefficients, using a least-squares fitting procedure. There are limitations to this approach, however, that are associated with the swelling level and the effect of stress. When swelling is low it is difficult to distinguish between and separate

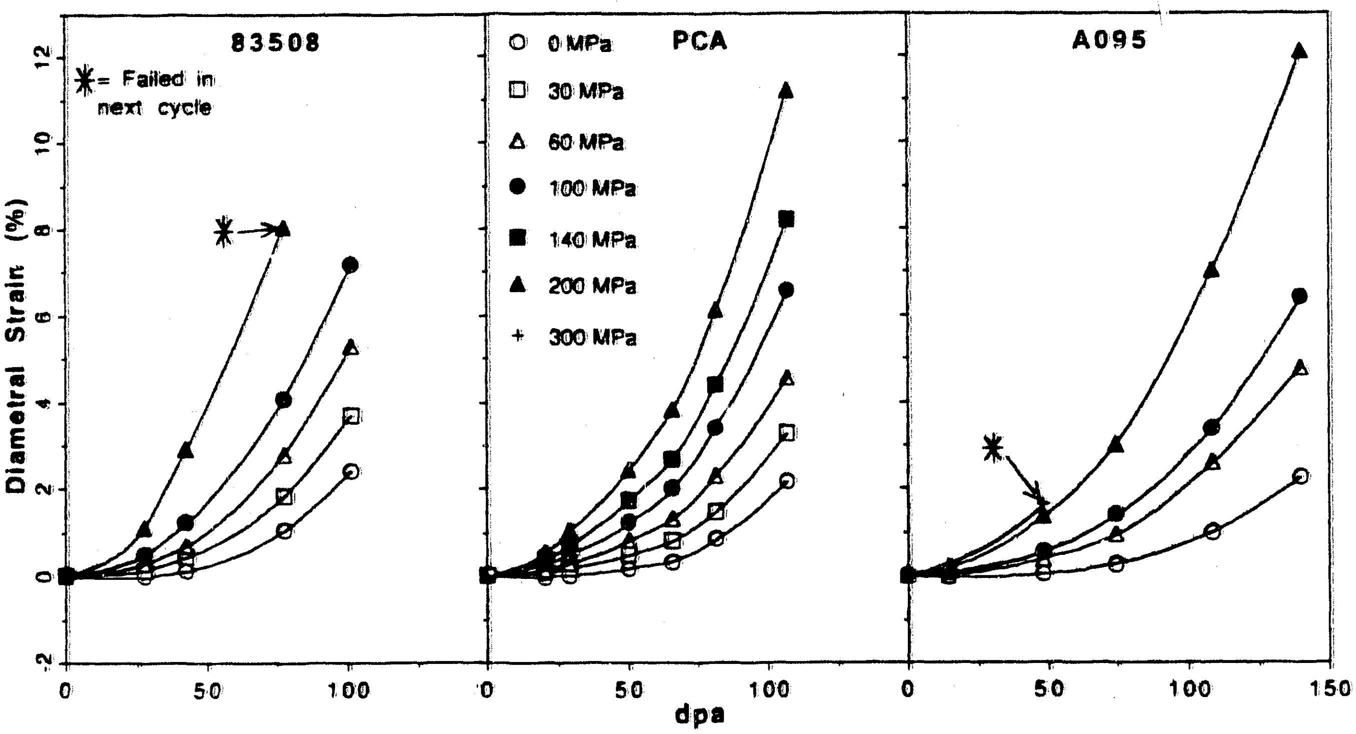

Figure 1. Creep and swelling strains observed in pressurized tubes made from three titanium-modified stainless steels that were irradiated in FFTF/MOTA at ~400°C.

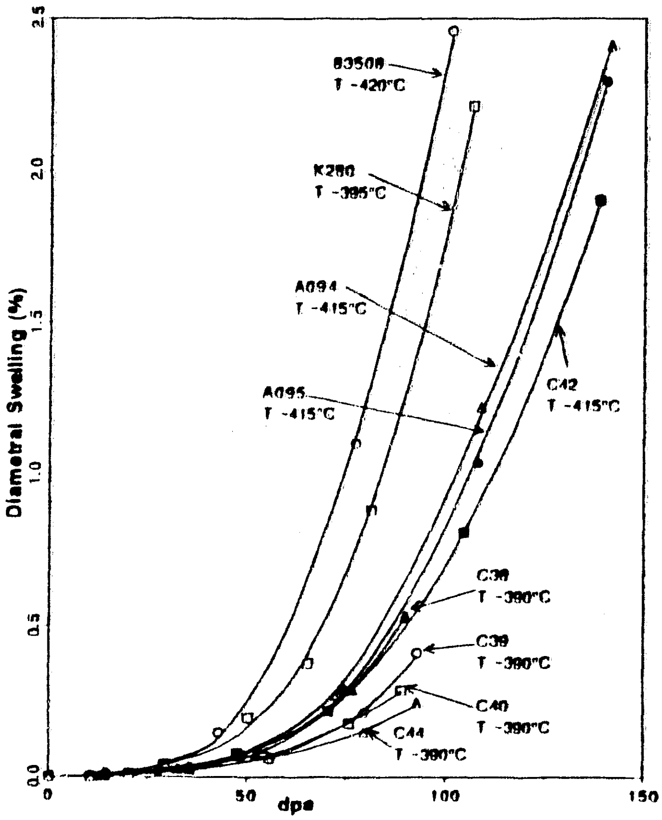

Figure 2. Dimetral strains resulting from void swelling at ~400°C in irradiated stress-free tubes constructed from nine titanium-modified stainless steels.

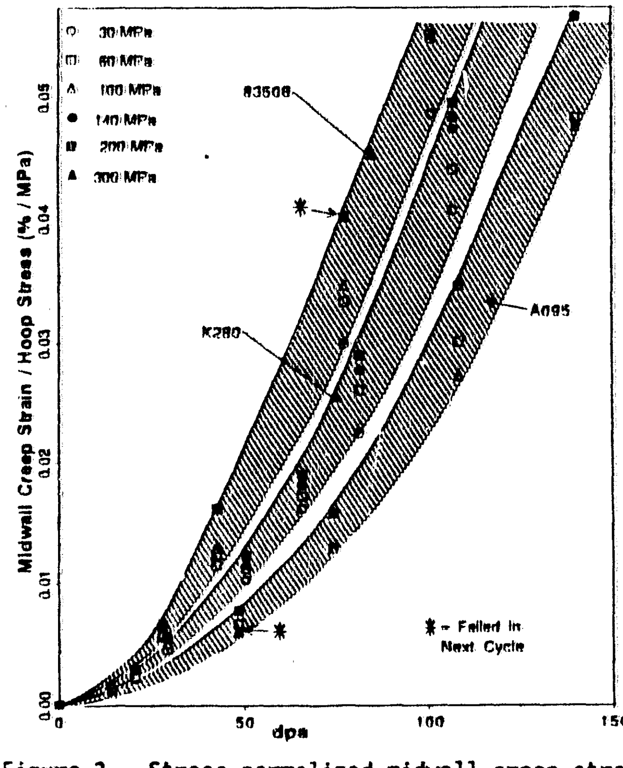

Figure 3. Stress-normalized midwall creep strains observed at ~400°C in three heats of titanium-modified stainless steels. Note that the creep strains develop in the same sequence as does the swelling of the various heats. The slight increase in normalized creep strains with stress level is thought to reflect the stress enhancement of swelling rather than a nonlinearity of creep rate with stress.

the B_o and $D\dot{S}$ contributions, especially when precipitation-related strains occur early in the irradiation. As swelling increases, the relative contribution of the non-swelling-related strains decreases and better estimates of the creep-swelling coupling coefficient become possible. It stress accelerates swelling it will appear that the B_o contribution is larger than it actually is.

The initial step of the first order estimation procedure is to fit the stress-free linear swelling strain (S_L) curve (Figure 2) with an equation of the form

$$S_L = \frac{a}{c} \log\left[\frac{(b + e^{-cx})}{(1 + b)\ e^{-cx}}\right], \tag{2}$$

where x is the dose in dpa, a is the steady-state swelling strain rate, b is the incubation parameter and c is a parameter controlling the rate of curvature between the incubation and steady-state regimes.

The second step is to fit each creep strain curve in Figure 3 with an equation of the form

$$\epsilon = qx + \frac{r}{c} \log\left[\frac{(b + e^{-cx})}{(1 + b)\ e^{-cx}}\right]. \tag{3}$$

Note that it is assumed that the incubation and curvature parameters are identical for both creep and swelling. This is a reasonable assumption if the B_o + DS model is correct. The degree of fit to the creep strain curves appears to confirm the validity of this assumption.

Upon integrating equation (1) with respect to x

$$\bar{\epsilon}/\bar{\sigma} = B_{ox} + DS + K. \tag{4}$$

where S ≈ $3S_L$ for small S_L. The parameter K = 0, since $\epsilon(0) = 0$ and $S(0) = 0$. When expressed in terms of midwall strain and hoop stress, σ_H, equation (4) becomes

$$\epsilon/\sigma_H = 3/4\ [B_o x + DS]. \tag{5}$$

Substituting equations (2) and (3) into equation (5) yields

$$\frac{qx}{\sigma_H} + \frac{r}{c\sigma_H} \log\left[\frac{(b + e^{-cx})}{(1 + b)\ e^{-cx}}\right] = \frac{3}{4} B_o x + \frac{9Da}{4c} \log\left[\frac{(b + e^{-cx})}{(1 + b)\ e^{-cx}}\right]. \tag{6}$$

Solving for B_o and D gives

$$B_o = \frac{4q}{3\sigma_H} \text{ and } D = \frac{4r}{9a\sigma_H}. \tag{7}$$

The least-squares fitting routines used to determine q, r, a, b and c starts from an initial graphical estimate of these values. Table 3 lists the first-order estimates of B_o and D calculated for each stress level and each alloy. For the PCA alloy, the coefficients were found to be -2×10^{-6} MPa^{-1} dpa^{-1} and -0.6×10^{-2} MPa^{-1}. The average values of these coefficients are also shown in table 3 and Figure 4 for all nine alloys. It appears that the values of D converge to 0.6×10^{-2} when the swelling level is sufficiently large, although significant variation can occur in the B_o term at convergence. The value of 0.6×10^{-2} MPa^{-1} for D in these titanium-modified steels agrees with that observed in the low titanium stainless steels (AISI 304 and AISI 316) at ~400°C, but the B_o values found in this study for the low titanium steels are somewhat higher than the usually assumed value of -1×10^{-6} MPa^{-1} dpa^{-1}. The larger values of B_o found in the titanium-modified steels are thought to be a possible consequence of lower levels of densification compared to the larger level of precipitate-related densification that occurs in low titanium steels where the carbon is not bound up in titanium carbides.[10]

Table 3. Calculated Values of the Creep Compliance, B_o, and the Creep-Swelling Coupling Coefficient, D

Heat	Stress level MPa		B_o, x10^{-6} MPa^{-1}dpa^{-1}	D, x10^{-2} MPa^{-1}
83508	30		3.1	0.46
	60		2.8	0.63
	100		3.3	0.57
	200		3.7	0.75
		Avg	3.2	0.60
K280	30		2.1	0.50
	60		2.2	0.57
	100		2.3	0.64
	140		2.4	0.60
	200		2.4	0.64
		Avg	2.3	0.59
A094	60		1.4	0.41
	100		1.4	0.40
	200		1.1	1.05
		Avg	1.3	0.62
A095	60		1.5	0.66
	100		1.4	0.65
	200		1.8	0.75
		Avg	1.6	0.69
C42	60		1.4	0.40
	100		1.6	0.56
	200		1.6	0.73
		Avg	1.5	0.56
C38	60		1.1	1.04
	100		1.3	1.19
	200		1.3	1.15
		Avg	1.2	1.13
C39	60		1.1	1.41
	100		1.2	1.37
	200		1.4	1.45
		Avg	1.2	1.41
C40	60		1.1	1.55
	100		1.0	1.74
	200		0.9	1.86
		Avg	1.0	1.72
C44	60		0.8	2.41
	100		0.8	2.63
	200		0.6	2.99
		Avg	0.7	2.68

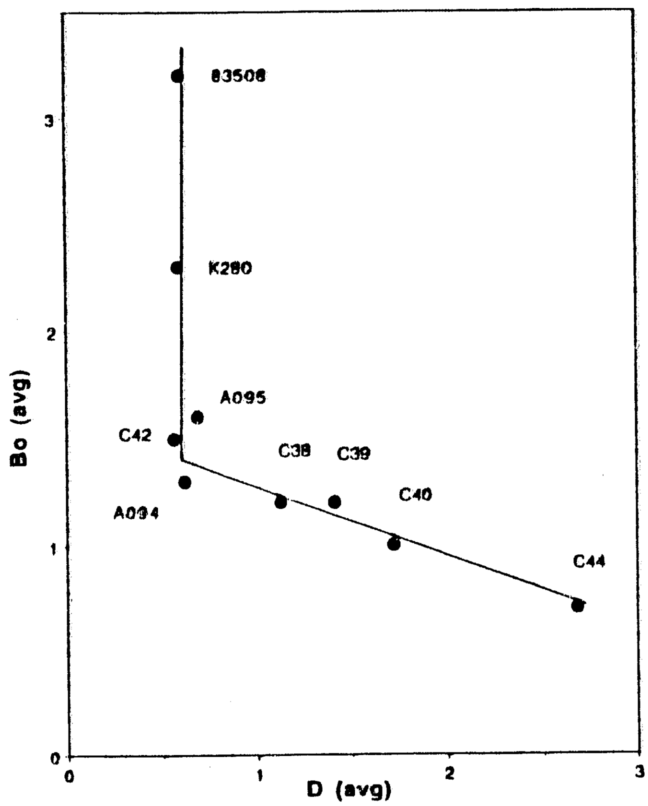

Figure 4. Calculated values of average creep compliance, B_o(avg), and average creep-swelling coupling coefficient, D(avg), for each alloy. Two regimes of behavior are observed. The data on the left hand vertical line describe alloys that exhibited a significant level of swelling. The other line describes irradiations in which the calculated value of B_o declines as the swelling level decreases. The lower derived values of B_o for these low swelling heats are accompanied by corresponding overestimates of the D coefficient.

Analysis of Data at Higher Temperatures

Both thermal creep and irradiation creep data from FFTF-MOTA are available for most of these steels at temperatures above 400°C. However, it is difficult to extract meaningful values of B_o and D from these higher temperature data. An overtemperature event in MOTA-1D for tubes irradiated at temperatures greater than 450°C resulted in a programmatic decision to terminate the irradiation of many of the high temperature tubes. At the lower fluence levels reached by these high temperature tubes, the swelling strains of titanium-modified steels were usually too low to provide separable estimates of the B_o and DS contributions.

In addition, thermal creep becomes a large contributor to the strain at the higher temperatures and tends to obscure the DS contribution to the total strain rate. An attempt is currently being made to derive estimates of B_o and D from other high temperature data sets that reached higher swelling levels in irradiation experiments conducted in both FFTF and EBR-II. The results of this analysis will be reported elsewhere.[19]

CONCLUSIONS

Based on the results of this and other studies on various austenitic stainless steels irradiated at ~400°C in either EBR-II or FFTF, it appears that the B_o + DS model of irradiation creep is valid for application as a design equation. This model can be applied to both PCA and austenitic steels in general, providing the effect of stress on swelling is relatively small. At ~400°C the value of D in the 300 series of steels appears to be ~0.6×10^{-2} MPa^{-1}, relatively independent of both composition and thermomechanical condition. Unfortunately, the data on titanium-modified steels available from FFTF at higher irradiation temperatures are insufficient at present to establish the temperature dependence of the creep-swelling coefficient.

ACKNOWLEDGEMENTS

M. B. Toloczko gratefully acknowledges support from the U.S. Department of Energy, Division of University and Industry Programs, Office of Energy Research, as a Science and Engineering Research Semester program participant at Pacific Northwest Laboratory.

REFERENCES

1. D. L. Porter, F. A. Garner and G. D. Hudman, "Irradiation Creep and Swelling of Annealed 304L Stainless Steel at ~390°C and High Neutron Fluence," Fusion Reactor Materials Semiannual Progress Report DOE/ER-0313/7 (1989) 133-139.

2. F. A. Garner, D. L. Porter and B. J. Makenas, J. Nucl. Mater. 148 (1987) 279-287.

3. D. L. Porter and F. A. Garner in Influence of Radiation of Material Properties, ASTM STP 956, Eds. F. A. Garner, C. H. Henager, Jr. and N. Igata (1987) 11-21.

4. F. A. Garner and D. L. Porter, J. Nucl. Mater. 155-157 (1988) 1006-1013.

5. D. L. Porter and F. A. Garner, J. Nucl. Mater. 159 (1988) 114-121.

6. R. W. Clark, A. S. Kumar and F. A. Garner, J. Nucl. Mater. 155-157 (1988) 845-849.

7. F. A. Garner, J. Nucl. Mater. 122-123 (1984) 459-471.

8. F. A. Garner and D. S. Gelles, J. Nucl. Mater. 159 (1988) 286-309.

9. K. Ehrlich, J. Nucl. Mater. 100 (1981) 149.

10. F. A. Garner, W. V. Cummings, J. F. Bates and E. R. Gilbert, "Densification-Induced Strains in 20% Cold-Worked 316 Stainless Steel During Neutron Irradiation," HEDL-TME 78-9, Hanford Engineering Development Laboratory, June 1978.

11. R. J. Puigh, A. J. Lovell and F. A. Garner, J. Nucl. Mater. 122-123 (1988) 242-245.

12. F. A. Garner, R. J. Puigh, M. L. Hamilton, M. B. Toloczko and A. S. Kumar in this semiannual report.

13. E. R. Gilbert and B. A. Chin in Effects of Radiation on Materials, Tenth Conference, ASTM STP 725, Eds. D. Kramer, H. R. Brager and J. S. Perrin, American Society for Testing and Materials, Philadelphia, (1981) 665-679.

14. M. B. Toloczko, F. A. Garner and C. R. Eiholzer, "Determination of Creep-Swelling Coupling Coefficients for Irradiated Stainless Steels," Fusion Reactor Materials Semiannual Progress Report DOE/ER-0313/9 (1991) 160-166.

15. F. A. Garner and R. J. Puigh, "Irradiation Creep of PCA Observed in FFTF/MOTA," Fusion Reactor Materials Semiannual Progress Report DOE/ER-0313/7 (1989) 140-144.

16. F. A. Garner, E. R. Gilbert and D. L. Porter, in Ref. 13 pp. 680-697.

17. T. Lauritzen, S. Vaidyanathan, W. L. Bell and W. J. S. Yang in Radiation-Induced Changes in Microstructure, 13th International Symposium (Part I) ASTM STP 955, F. A. Garner, N. H. Packan and A. S. Kumar, Eds., American Society for Testing and Materials, Philadelphia, 1987, pp. 101-103.

18. D. L. Porter, M. L. Takata and E. L. Wood, J. Nucl. Mater. 116 (1983) 272-276.

19. F. A. Garner and M. B. Tolozcko, in this semiannual report.

END

DATE FILMED

2 / 26 / 92